Available online at www.sciencedirect.com
ScienceDirect
C. R. Mecanique 335 (2007) 295–303
COMPTES RENDUS MECANIQUE
http://france.elsevier.com/direct/CRAS2B/

Melting and solidification: processes and models/Flows in solidification

Lattice Boltzmann method for melting/solidification problems

El Alami Semma [a,*], Mohammed El Ganaoui [b], Rachid Bennacer [c]

[a] *Université Hassan I, laboratoire de mécanique, FST de Settat, B.P. 577, Settat, Morocco*
[b] *Université de Limoges/CNRS, SPCTS, UMR CNRS 6638, 123, Albert-Thomas, 87000 Limoges, France*
[c] *Université de Cergy-Pontoise, laboratoire LEEVAM, 5, mail Gay-Lussac, Neuville-sur-Oise, 95031 Cergy-Pontoise cedex, France*

Abstract

The present work uses the Lattice Boltzmann method for solving solid/liquid phase change problems. The computed results demonstrate a good agreement with the existing benchmark solution for natural convection and with the experimental solution for solid/liquid interface interacting with the flow field. ***To cite this article: E. Semma et al., C. R. Mecanique 335 (2007).***

Résumé

Une méthode de type gaz sur réseau pour la transition solide/liquide. Il s'agit de montrer dans le présent travail la possibilité de traiter des problèmes de transition de phase solide/liquide par une approche de type gaz sur réseau. Les résultats illustrent un bon accord avec les résultats existants dans le cas d'écoulement de convection naturelle en cavité ainsi que dans le cadre d'un problème test de solidification dirigée. ***Pour citer cet article : E. Semma et al., C. R. Mecanique 335 (2007).***

Keywords: Computational fluid mechanics; Solid/liquid phase change; Lattice Boltzmann; Enthalpy method

Mots-clés : Mécanique des fluides numérique ; Changement de phase solide/liquide ; Gaz sur réseau ; Méthode enthalpique

Version française abrégée

Les méthodes dites Lattice Boltzmann (LB) ou de gaz sur réseau sont une classe d'approches pour particules mesoscopiques pour simuler les mouvements de fluides. Elles deviennent progressivement une alternative sérieuse aux méthodes traditionnelles pour la mécanique des fluides numérique [1–14]. Les méthodes LB sont particulièrement adaptées pour modéliser des écoulements autour des géométries complexes [8,9], et sont facilement mises en œuvre sur machines parallèles.

Historiquement, l'approche LB est développée à partir des gaz sur réseau, bien qu'elle puisse également être dérivée directement de l'équation simplifiée de Boltzmann [8]. En gaz sur réseau, les particules occupent les noeuds d'un réseau discret et transitent d'un nœud au prochain dans une phase de *propagation*. Puis, les particules se heurtent et obtiennent une nouvelle vitesse. C'est la phase de *collision*. Par conséquent la simulation progresse dans une alternance entre la collision et la propagation des particules.

* Corresponding author.
E-mail address: semmaalam@yahoo.fr (E. Semma).

1631-0721/$ – see front matter
doi:10.1016/j.crme.2007.05.015

Pour les problèmes de pure convection, on présente dans ce travail quelques validations avec le cas de la cavité couramment utilisée pour la qualification de codes numériques à faible vitesse [10] (Fig. 2).

On présente également une validation spécifique dans le cas de changement de phase (Fig. 3), ce type de validation de l'approche LB en présence de transition de phase n'a pas été relevé dans la littérature (au meilleur de notre connaissance). La Fig. 4 montre le champ dynamique et l'interface solide/liquide dans le cas test de Viskanta [16]. Les simulations basées sur la méthode LB montrent un bon accord avec les résultats expérimentaux.

Ensuite on illustre des situations particulières où la méthode permet de capturer un front de solidification en interaction avec des structures instationnaires dans une cavité contenant du Gallium et chauffée par le bas. Les auteurs ont déjà mis en évidence ces situations en utilisant une formulation enthalpique et une approximation numérique de type volumes finis [19–21]. La Fig. 5 montre le champ de vitesse et l'interface de transition de phase dans le cas de solidification dirigée par une technique de tirage (dite de Bridgman). Deux types de situations pouvant présenter un intérêt pour l'industrie de la croissance cristalline illustrent ceci. L'interface convexe/concave répondant à un écoulement symétrique affaibli au centre de la cavité et une interface concave répondant à un écoulement complexe intense au cœur de la cavité (Fig. 5).

L'intérêt de montrer le traitement de ce type de problème par des méthodes de type LB réside également dans l'extension possible à la prise en compte de la morphologie d'interface dans un calcul global de croissance cristalline [16–18].

1. Introduction

Computational Fluid Dynamics (CFD) simulations of complex flows, in particular for problems involving a phase transition, are generally based on space and temporal discretization of the differential equations describing the macroscopic state, i.e., solving a continuum mechanics formulation for the conservation equations. However, their solutions can be very difficult when considering complex geometries and moving boundaries and/or with multi-physics. This justifies the development of new routes of simulations such as Lattice Boltzmann approaches [1–14]. The main goal of these methods is being to model the fluid flow at the microscopic level in terms of local interactions between particles. Several advantages are apparent for these methods. For instance, the method should be easier with an intuitive treatment of particular conditions such as the presence of obstacles [8,9]. Moreover, the successive repetition of collisions and of propagations with the LB approach allows an easy computer implementation.

The history of using the LBM method for the simulation of phase change materials goes back to works by Miller and Miller et al. in 2001 [5,6]; they introduced the kinetic reaction equation as a model for phase change. The model successfully simulated the 2-D melting of Ga and the anisotropic growth of crystals into an undercooled melt. Miller et al. [7] extended the model to incorporate crystallization and surface tension effects. The method was applied to simulate binary alloy solidification. They also testified that dendritic growth into an undercooled melt showed a good agreement with the analytical results.

In this article, first, the developed scheme is applied to the classical natural convection in a square cavity and a good agreement was found by using traditional CFD methods [15]. Then the application to solidification/melting problems with its specificities is presented. A validation with Viskanta's results is given and then the simulation is extended to an unsteady melt interacting with the solid/liquid interface [16–18]. The interest of the LB treatment of such problem is the perspective for coupling with the interface morphology serving the global calculation including both macro and microscopic interactions neighboring the solid/liquid transition zone in the vicinity of the dendrites.

2. Model equations

2.1. Continuum medium formulation

It is important to remember the macroscopic equations before introducing LB method for melting and/or solidification problems.

Classically, the balance equations are derived from continuum media theory to describe transfers of mass, momentum and energy (and eventually species). These governing equations for natural convection with phase change can be written as follows:

$$\nabla \mathbf{V} = 0 \tag{1}$$

$$\frac{\partial \mathbf{V}}{\partial t} + (\mathbf{V}.\nabla)\mathbf{V} = -\nabla P + \nu \nabla^2 \mathbf{V} - g\beta(T - T_0) \tag{2}$$

$$\frac{\partial T}{\partial t} + \mathbf{V}.(\nabla T) = \alpha \nabla^2 T - \frac{L}{\rho C_p}\frac{\partial F_l}{\partial t} \tag{3}$$

where $\mathbf{V}$ is the velocity vector, P the pressure, ν the kinetic viscosity, α the thermal diffusivity, C_p the heat capacity and F_l the liquid fraction, L is the latent heat of phase change.

We assume constant properties (ν, α) and the Boussinesq approximation for density ρ: $\rho = \rho_0(1 - \beta(T - T_0))$, where ρ_0 and T_0 are the reference fluid density and temperature, respectively and β is the thermal expansion coefficient.

2.2. Lattice Boltzmann procedure

Lattice Boltzmann (LB) methods are a class of mesoscopic particle based approaches to simulate fluid flows. They are becoming a serious alternative or complementary to traditional methods for CFD [1–9]. LB methods are especially well suited to simulate flows in complex geometries, and they are straightforwardly implemented on parallel machines. Historically, the LB approach is developed from lattice gases, although it can also be derived directly from the simplified Boltzmann BGK equation. In lattice gases, particles live on the nodes of a discrete lattice. The particles jump from one lattice node to the next, according to their (discrete) velocity. This is called the *propagation* phase. Then, the particles collide and get a new velocity, the *collision* phase. Hence the simulation proceeds, alternating between particle propagations and collisions. The two phases can be clearly distinguished.

It can be shown that lattice gases lead to the Navier–Stokes equations of fluid flow [3,4]. The major disadvantage of the lattice gases method for common fluid dynamics applications was the exponential complexity of the collision rules which was overcome in previous works (see for instance [10–14]). If the main interest is a smooth flow field, one needs to average over a very large lattice and over a long time period. The LB method solves this problem by pre-averaging the lattice gas. It considers particle *distributions* that live on the lattice nodes, rather than the individual particles.

In the setting up, the velocity and thermal field have to receive a different treatment when considering the lattice approach [1–3].

2.2.1. LB equation for the velocity field

The Lattice Boltzmann method employed in this study uses an hexagonal lattice (Frisch–Hasslacher–Pomeau model) (Fig. 1), leading to the form:

$$f_i(\mathbf{x} + \mathbf{c}_i \Delta t, t + \Delta t) - f_i(\mathbf{x}, t) = \Omega_i \tag{4}$$

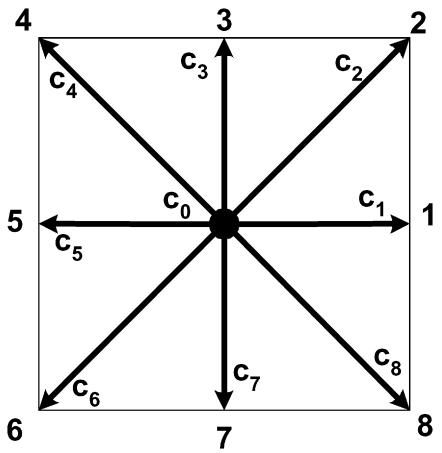

Fig. 1. Example of LB grid (D2Q9).

Fig. 1. Exemple d'une grille de type Lattice (D2Q9).

where f_i is the particle distribution defined for the finite set of the discrete particle velocity vectors $\mathbf{c}_i$. The collision term Ω_i on the right-hand side of Eq. (4) uses the so called Bhatangar–Gross–Krook (BGK) approximation. The essence of this approximation for LB method is that the collision term Ω_i will be replaced by the well-known classical single relaxation time:

$$\Omega_i = -\frac{f_i - f_i^{\mathrm{eq}}}{\tau} + \delta_i F_i \tag{5}$$

where τ is the relaxation time and f_i^{eq} is the local equilibrium distribution function that has an appropriately prescribed functional dependence on the local hydrodynamic properties. $\delta_i F$ is the external force field.

The equilibrium distribution can be formulated as in [4]:

$$f_i^{\mathrm{eq}} = \omega_i \rho\big(1 + 3(\mathbf{c}_i.\mathbf{u})/c^2 + 9(\mathbf{c}_i.\mathbf{u})^2/\big(2c^4\big) - 3\mathbf{u}.\mathbf{u}/\big(2c^2\big)\big) \tag{6}$$

where $\mathbf{u}$ and ρ are the macroscopic velocity and density, respectively, and the ω_i are the weights that are given by the length of the velocity vector:

$$\omega_0 = 4/9, \qquad \omega_{2k} = 1/36, \quad \omega_{2k+1} = 1/9; \quad k = 1, 2, 3, 4 \tag{7}$$

The set of discrete velocities $\mathbf{c}_i$ for the two dimensional and nine connected nodes (D2Q9) are defined as follows:

$$\mathbf{c}_0 = (0, 0), \qquad \mathbf{c}_{2k} = \sqrt{2}c\left[\cos\frac{(2k-1)\pi}{4}, \sin\frac{(2k-1)\pi}{4}\right],$$
$$\mathbf{c}_{2k+1} = c\left[\cos\frac{k\pi}{2}, \sin\frac{k\pi}{2}\right], \quad \text{for } k = 1, 2, 3, \ldots \tag{8}$$

where δx, δt and $c = \delta x/\delta t$ are the lattice size, time step and the lattice constant which depend on the lattice sound speed, respectively. The basic hydrodynamic quantities, such as density ρ and velocity $\mathbf{u}$, are obtained through moment summations in velocity space:

$$\rho(\mathbf{x}, t) = \sum_i f_i(\mathbf{x}, t) \tag{9}$$

$$\rho\mathbf{u}(\mathbf{x}, t) = \sum_i \mathbf{c}_i f_i(\mathbf{x}, t) \tag{10}$$

The Chapman–Enskog expansion for the density distribution function can recover the continuity and Navier–Stokes equations. The detailed derivation of this procedure is given in [13,14]. The lattice viscosity [3] is determined by:

$$\nu = \frac{1}{3}\left(\tau_v - \frac{1}{2}\right) \tag{11}$$

where τ_v is the relaxation time.

2.2.2. LB equation for the temperature field

In general, LB methods for a fluid flow involving heat transfer in a plain medium can be classified into two categories, the multi-speed models [3] and the double distribution function approach [4]. In the doubled population, the flow and the temperature fields are solved by two separate equations.

To derive the LBGK model for Eqs. (1)–(3), two LBGK equations are used to solve the velocity and temperature fields, respectively. In this context, the evolution equation for the internal energy is given as follows:

$$g_i(\mathbf{x} + \mathbf{c}_i\Delta t, t + \Delta t) - g_i(\mathbf{x}, t) = -\frac{1}{\tau_T}\big(g_i(\mathbf{x}, t) - g_i^{\mathrm{eq}}(\mathbf{x}, t)\big) \tag{12}$$

where g_i is the energy distribution function, τ_T is the dimensionless relaxation time for the temperature field, and the equilibrium temperature distribution function is given by:

$$g_0^{\mathrm{eq}} = -\frac{2}{3}e\rho\frac{\mathbf{u}.\mathbf{u}}{c^2}, g_{2k+1}^{\mathrm{eq}} = \frac{e\rho}{9}\left(\frac{3}{2} + \frac{3}{2}\frac{\mathbf{c}_{2k+1}.\mathbf{u}}{c^2} + \frac{9}{4}\frac{(\mathbf{c}_{2k+1}.\mathbf{u})^2}{c^4} - \frac{3}{2}\frac{\mathbf{u}.\mathbf{u}}{c^2}\right)$$
$$g_{2k}^{\mathrm{eq}} = \frac{\rho e}{36}\left(3 + 6\frac{\mathbf{c}_{2k}.\mathbf{u}}{c^2} + \frac{9}{2}\frac{(\mathbf{c}_{2k}.\mathbf{u})^2}{c^4} - \frac{3}{2}\frac{\mathbf{u}.\mathbf{u}}{c^2}\right) \quad \text{for } k = 1, 2, 3, 4 \tag{13}$$

the macroscopic temperature is calculated from:

$$\rho e = \sum_i g_i \tag{14}$$

The temperature and internal energy are related through the state equation, $e = RT$. The Chapman–Enskog expansion for the density distribution function recovers the macroscopic energy equation. This gives the thermal diffusivity α in term of the thermal single relaxation:

$$\alpha = \frac{1}{3}\left(\tau_T - \frac{1}{2}\right) \tag{15}$$

2.2.3. Phase change treatment

To solve the phase change problem, a fixed grid approach is used, similar to the principle used for enthalpy formulation when considering continuum media [19–22]. The melting process takes place over a temperature range $T_m \pm \varepsilon$, where ε is a small quantity (typically 5% of ΔT). The principle of the enthalpy method is to separate the sensible and latent heat components in the vicinity of the solid–liquid interface ($T_m - \varepsilon < T < T_m + \varepsilon$). The latent heat component is expressed in term of the latent heat and liquid fraction, F_l, which is defined as:

$$\begin{aligned} &F_l = 1 \quad \text{for } T > T_m + \varepsilon \\ &F_l = 0 \quad \text{for } T < T_m - \varepsilon \\ &F_l = (T - T_m + \varepsilon)/2\varepsilon \quad \text{for } T_m - \varepsilon \leqslant T \leqslant T_m + \varepsilon \end{aligned} \tag{16}$$

Dynamically, the phase change zone is treated like a porous medium. The flow penetration into the medium depends on its permeability. With the LB approach, this basic concept is introduced by assuming that the population densities are uniformly distributed throughout the volume of each node. Each particle moves a total distance of 1 or $\sqrt{2}$ lattice spacing in one time step, depending on its speed. If the node is totally solid, $f_\alpha^*(\mathbf{x}, t)$ is completely reflected. $f_\alpha(\mathbf{x}, t) = f_\alpha(\mathbf{x}, t + \Delta t)$. If the node contains a fraction of fluid $F_l \neq 1$, only a part of $f_i^*(\mathbf{x}, t)$ is propagated, the other part is reflected and returned to the initial cell.

We note f^{**} the result of the collision step given by:

$$f_\alpha^{**}(\mathbf{x}, t + \Delta t) = f_\alpha^*(\mathbf{x}, t) + \frac{1}{\tau}\left(f_\alpha^{\mathrm{eq}}(\mathbf{x}, t) - f_\alpha^*(\mathbf{x}, t)\right), \quad 0 \leqslant \alpha \leqslant 8$$

The streaming process in the porous media can be written as:

$$f_\alpha(\mathbf{x}, t + \Delta t) = f_\alpha^{**}(\mathbf{x}, t) + \lambda\left(f_{\bar{\alpha}}^{**}(\mathbf{x} + \mathbf{c}_\alpha \Delta t, t + \Delta t) - f_\alpha^{**}(\mathbf{x}, t + \Delta t)\right), \quad 0 \leqslant \alpha \leqslant 8$$

where $\bar{\alpha}$ is the index of the direction opposite $\mathbf{c}_\alpha$ and $\lambda = 1 - F_l$ a factor to take account of the permeability of the medium depending on the liquid fraction of the material in each node.

If $\lambda = 1$, there is no effect on streaming processes. if $\lambda = 0$, the streaming processes is reduced to the usual free-fluid LBM.

3. Results and discussion

3.1. Lattice versus the classical convection benchmark

To provide in this Note the complete LB ability to treat fluid flow interacting with phase change treatment, a first validation has been made with a commonly used test case of natural convection in a square cavity. The Prandtl number is fixed to $Pr = 0.71$ and the Rayleigh number is varied between 10^3 and 10^6; the LB solution is carried out by using the particle velocity model referred as the D2Q9 grid.

The LBM prediction was in good agreement with traditional CFD methods and published benchmark solutions for a range of tested *Ra* numbers [15]. Table 1 shows representative quantities of the flow field and heat transfer. Good agreement is found between LB results and classical based Navier–Stokes simulations. There are a little difference with the reference results, this is within 3% and can be considered acceptable for engineering applications.

Runs were performed on a 120×160 lattice grid. For low Rayleigh numbers, the heat transfer is dominated by diffusion and flow strength increases as *Ra* increases. At $Ra > 10^5$, the flow is characterised by distinct boundary layers adjacent to differentially heated walls. An illustration of temperature and flow patterns is given on Fig. 2 for $Ra = 10^6$.

Table 1
Results: present values (ϕ) and de Vahl Davis values [15] (ϕ)

Tableau 1
Résultats : cette étude (ϕ) et les valeurs de Vahl Davis [15] (ϕ)

Ra	u_{max}		v_{max}		Nu	
10^3	3.699	3.697	3.650	3.649	1.116	1.118
10^4	19.620	19.617	16.213	16.178	2.245	2.243
10^5	68.68	68.59	34.817	34.73	4.521	4.519
10^6	220.418	219.36	64.763	64.63	8.814	8.800

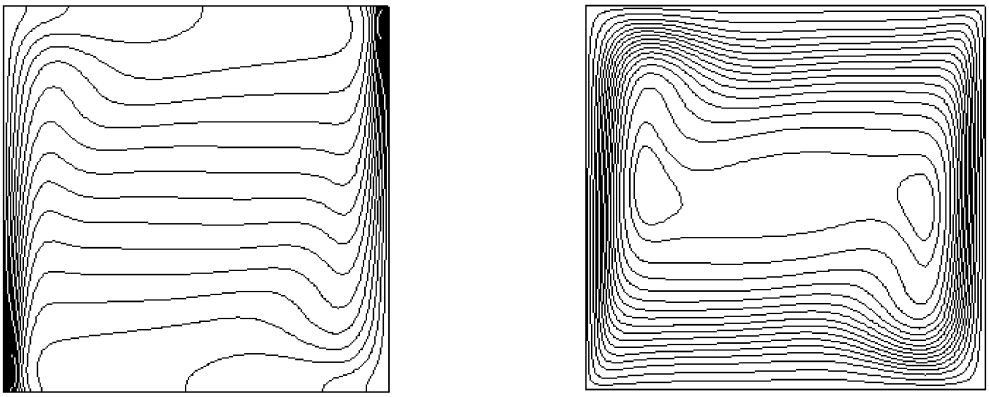

Fig. 2. Isotherms and streamlines for $Ra = 10^6$ (150 × 150 lattice grid).
Fig. 2. Illustration d'une simulation LB de convection pour $Ra = 10^6$ (maillage lattice 150 × 150).

3.2. Lattice extended to solid/liquid phase change

In recent years, there has been a growing interest in studying liquid metal flows in vertical Bridgman cavities as an academic and useful configuration for the process of solidification. When the fluid is heated from below, the flow exhibits a very strong and complex nonlinear behaviour. The Rayleigh–Bénard (RB) problems offer a first approach to understanding the flow/thermal complexity evolving from a conductive solution to a convective one. The LB method is applied to solve (RB) flows with phase change. A test case is then considered followed by a directional solidification. The test case refers to the Viskanta's experiments (widely cited for the verification of numerical codes). The experimental configuration is sketched in Fig. 3. Initially, a solid gallium block is kept at $T_i = 28.3\,^{\circ}\mathrm{C}$. The temperature at the bottom surface is increased suddenly to 38.0 °C, while the other walls are maintained in an adiabatic state. The Prandtl, the Rayleigh and the Stefan numbers are defined as:

$$Pr = \upsilon/\alpha = 0.021, \qquad Ra = g\beta\Delta T H^3/\upsilon\alpha, \qquad Ste = Cp\Delta T/L_f = 0.039$$

The predicted phase change fronts are illustrated in Fig. 4 and compared with the experimental data [16] and finite volume predictions [20]. The results are presented at $t = 12$ mn; we can conclude that there is a good agreement between the front calculated using LB method and experimental results.

For the practical application, the same cavity of aspect ratio $AR = L/H = 0.75$ and containing solid Gallium at the melting temperature is modelled. The temperature at the bottom wall is increased suddenly to $T = T_H$. The other walls are kept adiabatic. The heated conditions correspond to a high Rayleigh number ($Ra = 2 \times 10^6$).

At the beginning of the melt process, the interface shape remains planar. Thereafter, the melt zone size increases and the interface becomes deformed symmetrically with the development of the natural convection in the melt (Fig. 5(a)). The intensity of the flow increases with the increase of the melt depth size. Because of the asymmetric distribution of the convection cells the phase change interface becomes asymmetric (Fig. 5(b)), although the container geometry and

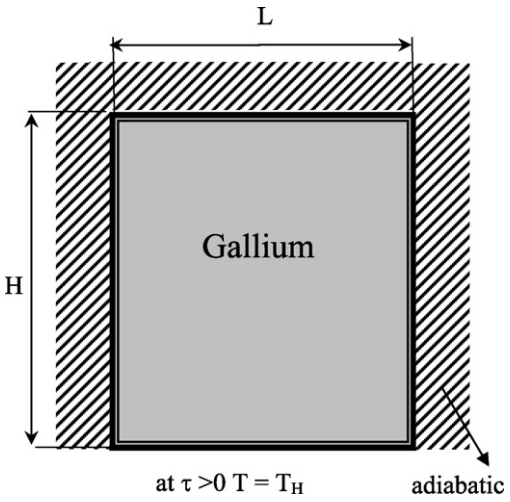

Fig. 3. Schematic of the computed domain.

Fig. 3. Problème test pour changement de phase.

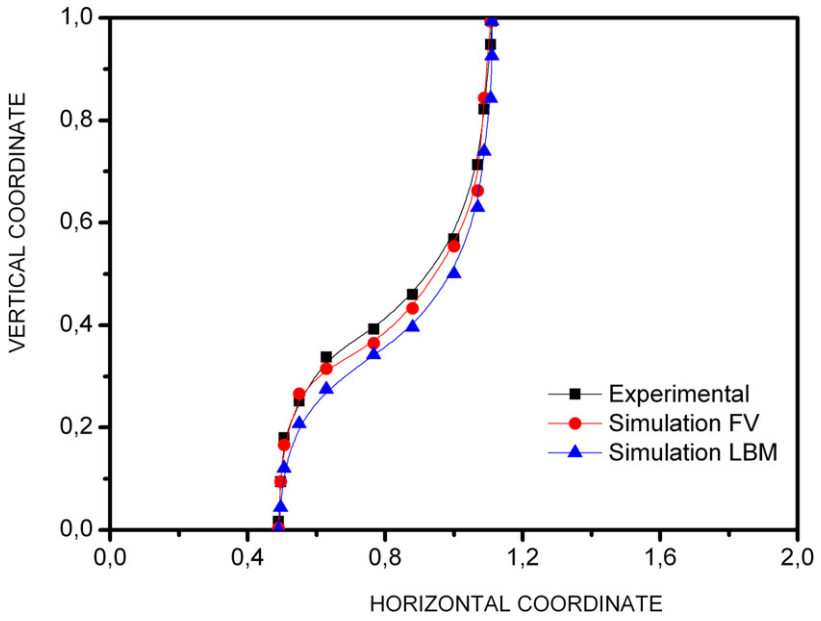

Fig. 4. Comparison of the predicted solid/liquid interface with experimental data [16] and finite volume method [20] (120 × 240 lattice grid).

Fig. 4. Résultat LB pour l'interface comparée aux résultats expérimentaux [16] et à une simulation VF [20] (maillage lattice 120 × 240).

the boundary conditions are symmetric, i.e., symmetry breaking phenomena take places as the controlling parameter, *Ra*, increases. The isotherms are closer in the bottom region where the flow is directed towards the bottom wall, indicating the presence of an intense flow in this area. These observed patterns can principally illustrate the ability of LB to follow complex fluid solution under phase change coupling. An extended work focusing on unsteady tracked lattice solution is under finalisation by the authors [22].

4. Conclusion

This article provides an illustration of treating coupled phase change/convection problems using a Lattice Boltzmann approach.

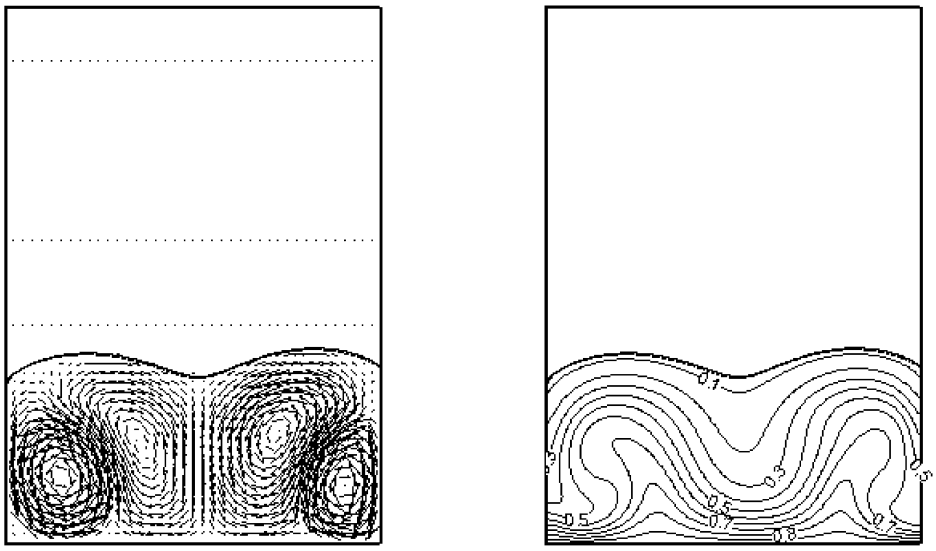

(a) *t= 12 s*

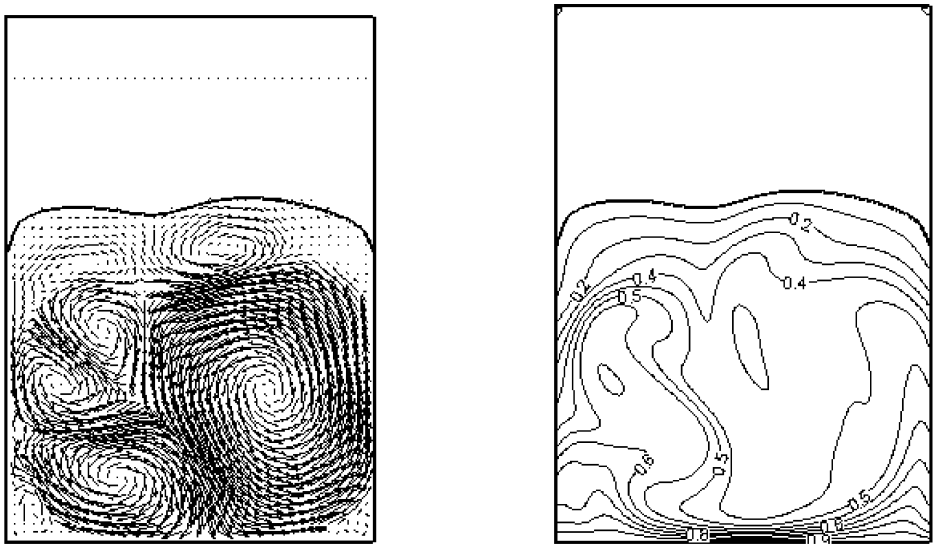

(b) *t= 28 s*

Fig. 5. Velocity vectors (left) and Isotherms (right) with solid/liquid interface for $Ra = 2 \times 10^6$ at $t = 12$ s and $t = 28$ s (120×160 lattice grid).

Fig. 5. Résultats LB pour champ dynamique complexe en interaction avec l'interface (a) et lignes isothermes (b) pour $Ra = 2 \times 10^6$ à $t = 12$ s et $t = 28$ s (maillage lattice 120×160).

A first comparative case refers to the well-known benchmarking exercise. The last case shows the ability of the LB approach to describe complex fluid flow in a directional solidification cavity. Interface deformations are also simulated. Such scheme can be easily extended to consider the interface morphology with dendritic growth, local micro-flows and local solidification structures, leading onto developing global simulation codes coupling the micro/macro aspect in 3D configurations and implemented in a straightforward manner.

Acknowledgements

The authors would like to express their gratitude to Professor A.A. Mohamad from the University of Calgary for fruitful discussions on LB methods during his visit to the University of Limoges.

References

[1] M. Jami, A. Mezrhab, M. Bouzidi, P. Lallemand, Lattice-Boltzmann computation of natural convection in a partitioned enclosure with inclined partitions attached to its hot wall, Physica A: Statist. Mech. Appl. 368 (2) (2006) 481–494.

[2] A. Mezrhab, M. Jami, C. Abid, M. Bouzidi, P. Lallemand, Lattice-Boltzmann modelling of natural convection in an inclined square enclosure with partitions attached to its cold wall, Int. J. Heat Fluid Flow 27 (3) (2006) 456–465.

[3] F.J. Alexander, S. Chen, J.D. Sterling, Lattice Boltzmann thermohydrodynamics, Phys. Rev. E 47 (1993) R2249.

[4] X. He, S. Chen, G.D. Doolen, A novel thermal model for the lattice Boltzmann method incompressible limit, J. Comput. Phys. 146 (1998) 282–300.

[5] W. Miller, The lattice Boltzmann method: a new tool for numerical simulation of the interaction of growth kinetics and melt flow, J. Crystal Growth 230 (2001) 263–269.

[6] W. Miller, S. Succi, D. Mansutti, Lattice Boltzmann model for anisotropic liquid–solid phase transition, Phys. Rev. Lett. 86 (16) (2001) 3578–3581.

[7] W. Miller, I. Rasin, F. Pimentel, Growth kinetics and melt convection, J. Crystal Growth 266 (2004) 283–288.

[8] S. Succi, The Lattice Boltzmann Equation for Fluid Dynamics and Beyond, Clarendon Press, Oxford, 2001.

[9] C.K. Chen, T.S. Yen, Y.T. Yang, Lattice Boltzmann method simulation of backward-facing step on convective heat transfer with field synergy principle, Int. J. Heat Mass Transfer 49 (2006) 1195–1204.

[10] F.J. Higuera, J. Jimenez, Boltzmann approach to lattice-gas simulations, Europhys. Lett. 9 (7) (1989) 663–668.

[11] F.J. Higuera, S. Succi, R. Benzi, Lattice gas dynamics with enhanced collisions, Europhys. Lett. 9 (1989) 345–349.

[12] F.J. Benzi, S. Succi, M. Vergassola, The lattice Boltzmann equation: theory and applications, Phys. Rep. 222 (1992) 145–197.

[13] S. Hou, Q. Zou, S. Chen, G. Doolen, A.C. Cogley, Simulation of cavity flow by the lattice Boltzmann method, J. Comput. Phys. 118 (1995) 329–347.

[14] B.I. Pavel, A.A. Mohamad, A numerical study on vortex shedding from two side by side cylinders using the lattice Boltzmann method, in: R. Bennacer, M. El Ganaoui, A.A. Mohamad, J. Sicard (Eds.), Progress in Computational Heat and Mass Transfer, vol. I, Lavoisier-Tec & Doc., 2006, pp. 411–416.

[15] G. de Vahl Davis, Natural convection of air in a square cavity: a benchmark numerical solution, Int. J. Numer. Fluid Meth. Fluids 3 (1983) 249–264.

[16] C. Gau, R. Viskanta, Melting and solidification of a metal system in a rectangular cavity, Int. J. Heat Mass Transfer 27 (1984) 113–123.

[17] F. Wolff, R. Viskanta, Solidification of pure metal at a vertical wall in the presence of liquid superheat, Int. J. Heat Mass Transfer 31 (1988) 1735–1744.

[18] J.E. Simpson, R.S. Garimella, An investigation of solutal thermal and flow fields in unidirectional alloy solidification, Int. J. Heat Mass Transfer 41 (1998) 2485–2502.

[19] M. El Ganaoui, A. Lamazouade, P. Bontoux, D. Morvan, Computational solution for fluid flow under solid/liquid phase change conditions, Int. J. Comput. Fluids 31 (4–7) (2002) 539–556.

[20] E. Semma, Etude numérique des transferts de chaleur et de masse durant la croissance dirigée : effet de paramètres de contrôle, Thèse de doctorat Franco-Marocaine, Université de la Méditerranée/Université Mohamed V, 2004.

[21] J. Kaenton, E. Semma, V. Timchenko, M. El Ganaoui, E. Leonardi, G. de Vahl Davis, Effects of anisotropy and solid/liquid thermal conductivity ratio on flow instabilities during inverted Bridgman growth, Int. J. Heat Mass Transfer 47 (2004) 3403–3413.

[22] E. Semma, M. El Ganaoui, R. Bennacer, A.A. Mohamad, Melting and solidification problem, the lattice Boltzmann method, Int. J. Thermal Sci. (2007), in press.